



System for Diagnosing Main Pipelines of Heat Networks Based on UAVs

Artur ZAPOROZHETS

Institute of Engineering Thermophysics of NAS of Ukraine, Kiev, Ukraine,
e-mail: a.o.zaporozhets@nas.gov.ua

Abstract

The possibilities of thermal aerial photography for detecting different types of defects on pipelines in a functioning state are explored. The characteristics and capabilities of the proposed set of devices for monitoring thermal losses in pipelines based on quadcopters are considered. The created hardware-software complex for diagnosing the state of trunk pipelines of heat networks based on the UAV is considered. The obtained experimental results, confirming the possibility of differences in the technical condition of pipelines.

Keywords: UAV, main pipeline, heat networks, diagnostics, thermal aerial photography, hardware

1. Introduction

In modern conditions, district heating systems in the Nordic countries reach a level of 60%, and in the CIS countries – 80% of all systems that supply heat energy to residential, public and industrial buildings and structures. One of the main advantages of district heating systems is the possibility of using such types of fuel that are optimal in a technical and economic point of view and provide a greater ecological purity of the environment [1].

The main means of transporting thermal energy in the centralized heat supply are steel pipes with different types of insulation, and the prevailing methods of laying pipelines in cities are underground. [2] These pipelines with the necessary equipment form the heat network.

In Ukraine, one of the world's highest saturation of cities with heat networks, while the total length of pipelines is about 47 thousand km. More than 20 thousand km of pipes with a diameter from 50 to 800 mm are on the balance of municipal heat power engineering enterprises. In most cases, the ducts of heat pipelines are not protected from the penetration of soil water and other moisture, which leads to significant losses of thermal energy, corrosion damage to the metal of pipes and emergency shutdown of consumers. The total heat loss in the functioning networks of district heating systems is about 30%. The term of trouble-free operation of such networks does not exceed 10-15 years.

Replacing damaged pipelines will solve the problem of significant heat loss during its transportation to the final consumer, but at the moment this is not possible due to the economic situation. The only way out of the current situation is to monitor the technical condition of heating networks (especially trunk pipelines), timely detection of critical defects of such systems and their early elimination.

2. Features of thermal aerial photography

There are many methods for diagnosing the technical condition of heat and power facilities [3, 4, 5, 6]. Thermal imaging is the registration of electromagnetic radiation from objects of control in the infrared range and its transformation into a visible image.

Thermal aerial photography at the moment is the only way that in short periods of time allows to identify emergency and potentially defective sections of pipelines of heat networks [7, 8, 9].

With its help, it is possible to promptly examine large areas of the urban landscape and with high confidence to record the anomalous parts of the temperature field on the unpaved surface [10, 11, 12].

Typically, thermal aerial photography is performed at an altitude of 300-400 m along a system of parallel routes with an inter-route distance of 300-500 m, which provides at least 40% of the image overlap to obtain a picture of the distribution of thermal energy on the plane [13, 14, 15]. Thermal aerial photography is performed in early spring or late autumn in the absence of snow cover, when the heating networks are in operation mode. To eliminate distorting thermal effects from solar insolation, aerial photography should be carried out at night, less often during the daytime with high overcast clouds [16, 17, 18]. Aerial photography is not carried out with fog, precipitation and wind speed of more than 10 m/s.

Hidden places of leakage of the heat carrier, zones of destruction of thermal insulation, areas of flooding of heat pipes are confidently fixed on thermograms obtained during thermal aerial photography [19, 20, 21] (Fig. 1).



Fig. 1. A snapshot of the residential area obtained during the thermal aerial photography

The studies carried out at the Institute of Technical Thermophysics of the National Academy of Sciences of Ukraine suggest that the method of thermal aerial surveys is able to diagnose the technical condition of the main pipelines of heat networks (Table 1).

3. Features of the processing of thermal images

The development of algorithms is based on quality and speed of execution with high accuracy and low computational costs. Based on these requirements, the algorithm can be constructed according to the following logic [22]:

- thermal imaging (color) image is converted to black-white format (rank 0). In grayscale, the black-white image pixel values are in the range from 0 to 255 (0 is black, 255 is white);
- to reduce the computation time and cut off extraneous noise on the image, the pixel values are in the [0,127] range by a logical right shift by one bit;
- reduction of the image to rank 1 (reduction of the image in length and width by 2 times);
- application to the image of the convolution operator or the Laplace operator;
- calculation of the threshold;

- binarization and selection of object boundaries.

Next will be considered the input thermal image of rank 0, obtained from the thermal imaging device. If its dimensions are 640x480 (307200) pixels, then transformation to rank 1 will give an image with dimensions of 320x240 (76800) pixels.

The color image is brought to grayscale by any of the known methods:

1. according to the CCIR-601 standard

$$F[y, x] = 0.299R + 0.587G + 0.114B; \quad (1)$$

2. by the arithmetic mean value of the color components of the three channels

$$F[y, x] = (R + G + B)/3; \quad (2)$$

3. fast (using an algorithm with green pixels)

$$F[y, x] = G. \quad (3)$$

where R – red, G – green, B – blue (digital image components).

Further, it is rational to treat the image as a rectangular matrix of the size of $n \times m$ elements, the values of which are cut in the range from 0 to 127. The leading digit is sign, equal to zero, all values of the matrix are positive. Matrix filters are used to solve the problems of image preprocessing that perform the convolution operation, which allows to obtain response values, taking into account the values of the surrounding pixels, within the dimension of the core. This filter matrix is also called a convolution kernel — usually a square matrix of $n \times n$ elements, where n is odd. Various matrix filters are used to perform smoothing, remove noise in images, enhance clarity, highlight margins. Most of them have a dimension of 3x3 elements. For highly noisy thermal images, it is necessary to use relatively large masks. An example of such a discrete diagonal Laplacian with an 11x11 element filter is given in [23].

Further, the central element of the filter is superimposed on the studied pixel. The remaining elements are also superimposed on neighboring pixels. Next, the sum is calculated, where the terms are the multiplied values of the pixels and the values of the cell of the core that covered the given pixel:

$$G[y, x] = \left(\sum_{dy=-5}^5 \sum_{dx=-5}^5 (F^i [y + dy, x + dx] \times D_{y,x}^2 [dy, dx]) \right) shr2, \quad (4)$$

where F^i – rank matrix $I \in [0, 1]$, $shr2$ – operation of logical shift right by two digits.

Table 1. Assessment of the state of the main heating networks using UAVs

Type	Heat loss (%)	Characteristic
Normalized heat losses	5-10	Dry and integral insulation of pipelines, minimum heat flow from the coolant to the earth's surface
Increased heat loss	10-15	Wet or broken insulation of pipelines, which contributes to the nucleation of corrosive damage; in the thermal field can be displayed by a clear anomaly of the average brightness level and an increased width of the thermal trace
High heat losses	15-20	Damaged and damp insulation of pipelines, the canal is often filled with water from neighboring water pipelines with groundwater or melt water; in the thermal field is displayed as a high-contrast anomaly with a width several times larger than normal

Emergency condition	>20	Abnormalities of the thermal field have very high contrast and a broad indistinct shape due microrelief features
---------------------	-----	--

A logical shift to the right by two bits (division by 4) of the result of the convolution is made to bring it into the range $[-32768, 32767]$, what twice reduces the amount of necessary memory and allows to get rid of the reaction to noise in the image. The greater the dimension of the convolution kernel, the more accurate the response can be expected from the current pixel, since the set of neighboring pixels are also involved in the convolution operation, which leads to a large number of calculations.

Image processing by 11×11 filter implies a large number of multiplication operations, and there are two-digit numbers in this matrix, which will lead to an increase in time to calculate the value of one response. As a result, to reduce the computational cost, approximately 3 times, instead of the 11×11 operator, you should use an operator with a kernel size of 7×7 elements and then double the operator with a core of 3×3 elements, which will give an equivalent result when processed by one 11×11 operator.

The method of competitive analysis gives a good result for pattern recognition on non-noisy images. However, in the conditions of noise, poor visibility or the presence of foreign objects it is also possible to apply the contour method using masks of a higher dimension, as well as introducing the definition of “singular points” – extreme response values on such images.

To determine the specific points, the algorithm of the Moravec detector is used as a basis, which compares the extremes at the corners of the image using local detectors. A black-white image arrives at the detector input. At the output, a matrix is formed with elements whose values determine the degree of plausibility of finding the angle in the corresponding pixels of the image. The threshold value allows to “drop” the pixels, the degree of likelihood of which is less than the threshold. The remaining points are special or extremes. The Moravec detector is a simple angle detector, estimating the change in pixel intensity (y, x) by offsetting a square window centered in the current pixel (y, x) by one pixel in each of the 8 directions. This method is implemented as follows:

- for each direction of displacement

$F(u, v) \in \{(1, 0), (1, 1), (0, 1), (-1, 1), (-1, 0), (-1, -1), (0, -1), (1, -1)\}$, the change in intensity is calculated

$$V_{u,v}(y, x) = \sum_{\forall a,b} (I(x+u+a, y+v+b) - I(x+a, y+b))^2, \quad (5)$$

where $I(x+a)$ is the intensity of a pixel with coordinates (y, x) in the source image;

- builds a map of the probability of finding the angles in each pixel of the image by calculating the estimated function. Essentially, the direction is determined, which corresponds to the smallest change in intensity, because the corner must have adjacent edges;
- pixels are cut off, in which the values of the evaluation function are below a certain threshold value;
- recurring corners are removed using the NMS procedure (non-maximal suppression);
- non-zero elements correspond to the angles in the image.

The use of the Moravec detector makes it possible not to calculate the change in intensity, but to immediately perform an analysis on the generated response matrix. The table of directions will determine the maximum and minimum values of the response value located in the center of the window:

$$f = \begin{cases} G[y, x] > 0 \text{ AND } G[y, x] > G[y+dy, x+dx] \\ G[y, x] < 0 \text{ AND } G[y, x] < G[y+dy, x+dx] \end{cases} \quad (6)$$

for all extremums $dy = dx \in [-1; 0)$ AND $(0, 1]$. Extremes can be in maximum proximity to each other through one element of the response, therefore, in order to reduce the number of iterations when an extremum is found, the following, in the direction of the sweep, the value is excluded from the comparison procedure.

4. Hardware of diagnostic system

To carry out experimental studies of the monitoring system of the technical condition of heat pipelines, a multi-rotor type unmanned aerial vehicle, model MJX BUGS 3, was used.

The MJX BUGS 3 quadcopter (Fig. 2) is a world-renowned radio control toy manufacturer Meijiixin Toys. The company is positioning this drone designed for both aerial photography and dynamic flights.



Fig. 2. MJX BUGS 3

The features of this quadcopter include:

- support for 3S batteries;
- control of battery charge and flight distance;
- long flight time;
- axle suspension;
- control at 2.4 GHz;
- 360° flip;
- LED-backlight.

The quadcopter case MJX BUGS 3 is made of nylon fiber, has established itself as a reliable and durable material, while the supports are made of ordinary plastic.

The quadcopter MJX BUGS 3 is equipped with brushless motors of type MT1806 with a capacity of 1800kv. The manufacturer describes them as economical and efficient among the same type of brushless motors. Each motor provides 230 grams of traction.

Also in quadcopter available speed controllers ESC with automatic anti-jamming, eliminating the possibility of burnout engines.

Included with the drone is a axle-free suspension with manual vertical adjustment, adapted for installing a small load. The distance from the ground to the suspension is 80 mm.

The quadcopter is powered by a 2S Li-Po battery with a capacity of 1800 mAh with a discharge current of 25C and an XT30 connector. According to the specification, the battery provides 19 minutes of continuous flight.

The quadcopter kit also includes hardware operating at 2.4 GHz. Its distinctive feature is the function of intelligent remote control, reports a low battery or a long distance of the drone from the equipment. It is powered by 4 AA batteries. The maximum distance of the drone from the equipment is 300-500 meters.

During flight tests, the MJX BUGS 3 shows good flight performance even on the type 2S battery included in the kit. The 6-axis gyroscope works smoothly. In practice, the flight time of the quadcopter with a maximum load was 8 minutes. At a distance of 300 meters, the quadcopter clearly performs the specified flight directions

The main advantages and disadvantages of the quadcopter MJX BUGS 3 are shown in Table 2.

Table 2. Advantages and disadvantages of the model MJX BUGS 3

Advantages	Disadvantages
ease of use power feedback function with low charge and critical distance suspension for cargo compatible with 3S-batteries LED backlight price	lack of dynamism charged battery as standard

To perform experiments with thermal imaging of heat supply pipelines on the basis of the UAV, a compact thermal imaging camera manufactured by Seek Thermal™ (USA) (Fig. 3) was installed, which has a wide-angle lens with a total size of 2.5 x 4.4 x 2.5 cm resolution of 320 x 240. The greatest shooting distance is 610 meters, and the closest distance is 15 cm.



Fig. 3. XR Compact thermal imaging camera (Seek Thermal)

The appearance of the diagnostic system of main pipelines of heat networks is shown in Fig. 4.

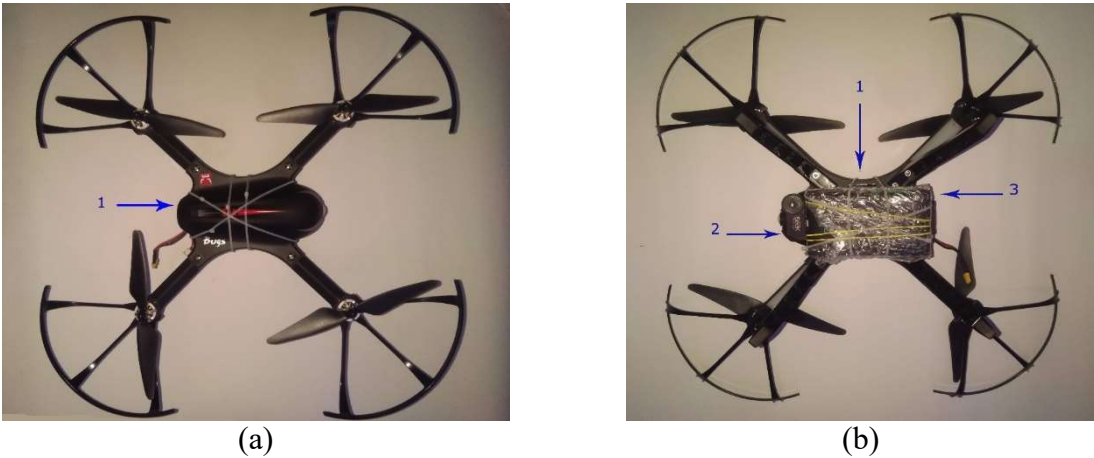


Fig. 4. Hardware complex for monitoring the technical condition of main pipelines:
 a) top view; b) bottom view;
 1 – UAV, 2 – thermal imaging camera; 3 – communication device

5. Experimental research

For monitoring extended objects (in our case, pipelines of heat networks) it is proposed to fly around the test object using a multi-rotor type UAV. This allows you to get high-quality photos and thermal images of the site of the heating system as an object of control for further analysis. The software allows you to use any topographic basis as a map. Binding can be done at two or more points. It is also possible to use as a topological basis of electronic maps. The program provides input, automatic control and editing of the route of the flight. An elevation can be specified for each waypoint.

The results of measuring the thermal state of the heat grids were carried out using a thermal imaging camera, mounted on a UAV.

Fig. 5 shows thermal images of sections of the heat network where experimental studies were conducted. The shooting was performed on November 22, 2018 at 18 p.m. on a cloudless sky at an air temperature of $-4\text{ }^{\circ}\text{C}$.

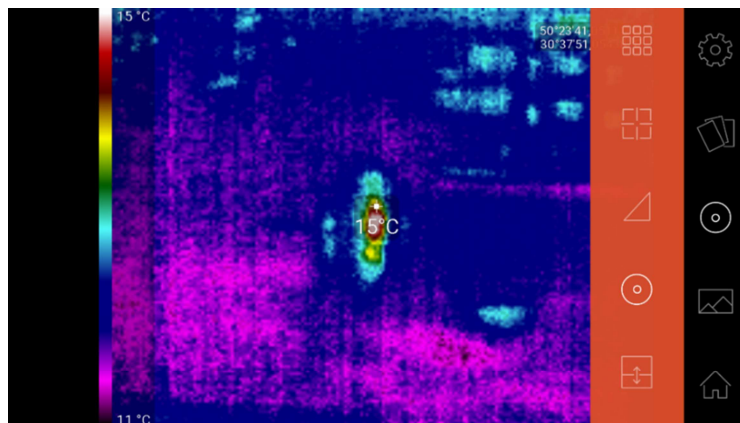


Fig. 5. The working environment of the software complex based on Seek Thermal

Fig. 5 clearly shows the possibility of identifying defective areas of main pipelines using low power UAVs.

6. Conclusions

Today we can state the rapid development of UAVs, which are mainly used in military operations. The list of subject areas of the use of UAVs for various other studies, operations, conventionally called non-military, is essentially limited. First of all, this limitation is due to the lack of created, developed and manufactured technical tools for conducting diverse studies, primarily measuring tools. It can be predicted that such an imbalance will soon be broken and the process of creating appropriate equipment for the UAV will be adjusted to conduct a wide range of research in various subject areas, among which the defense industry of the states will be priority and prospective.

The creation of mobile information-measuring systems based on UAVs makes it possible to diagnose the state and dynamics of the characteristics in time and space of the studied environment, both in on-line modes and other modes. The on-line mode is especially effective in case of accidents in areas of spatially branched heat networks. With normal operation of the objects under study, the current remote control is the most economical compared with other means of control. This allows to use such measuring tools to create the necessary databases for diagnostics the characteristics of the thermal state of heat networks to predict their dynamics.

References

1. Babak V., Zaporozhets A., Kovtun S., Sergienko R. Diagnosing methods analysis of bulk heating systems technical condition. *The Scientific Heritage*. Vol. 1, No. 14, 2017, pp. 59-65.
2. Babak V., Zaporozhets A., Kovtun S., Serhiienko R. Methods and Means of Heat Losses Monitoring for Heat Pipelines. *International Journal "NDT Days"*. Vol. 1, No. 2, 2018, pp. 213-221.
3. Slippey A, Ellis M., Conway B., Yun H. Heat Pipe Embedded Carbon Fiber Reinforced Polymer Composite Enclosures for Avionics Thermal Management. *SAE Technical Paper*. 2014-01-2189, 2014
4. Zaporozhets A., V. Eremenko, R. Serhiienko R., Ivanov S. Development of an Intelligent System for Diagnosing the Technical Condition of the Heat Power Equipment. *IEEE 13th International Scientific and Technical Conference on Computer Sciences and Information Technologies (CSIT)*. 2018, pp. 48-51. doi: 10.1109/STC-CSIT.2018.8526742
5. Zaporozhets A., Eremenko V., Serhiienko R., Ivanov S. Methods and Hardware for Diagnosing Thermal Power Equipment Based on Smart Grid Technology. *Advances in Intelligent Systems and Computing III*. Vol. 871, 2019, pp. 476-489. doi: 10.1007/978-3-030-01069-0_34
6. Babak V.P., Kovtun S.I. Calibration thermoelectric heat flux sensor in the diagnostic system of thermal state of electric machines. *Tekhnichna elektrodynamika*. №1, 2019, pp. 89-92.
7. Dimov D., Velinov K. Application Fields of the Thermal Imaging Method. *International Journal "NDT Days"* Vol. 1, Issue 2, 2018, pp. 145-154.
8. Zaporozhets A. Analysis of methods for diagnosing heat energy objects. *Science-based technologies*. Vol. 35, No. 3, 2017, pp. 259-265. doi: 10.18372/2310-5461.35.11846
9. Babak V., Zaporozhets A., Sverdlova A. Smart Grid Technology in Monitoring of Power System Objects. *Industrial Heat Engineering*. Vol. 38, No. 6, 2016, pp. 71-81. doi: 10.31472/ihe.6.2016.10
10. Anweiler S., Piwowarski D., Ulbrich R. Unmanned Aerial Vehicles for Environmental Monitoring with Special Reference to Heat Loss. *International Conference Energy, Environmental and Material Systems (EENS 2017)*. Vol. 19, 2017.
11. Zaporozhets A., Sverdlova A. Peculiarities of application of Smart Grid technology in systems for monitoring and diagnostics of heat-and-power engineering objects. *Technical Diagnostics and Non-Destructive Testing*. No. 2, 2017, pp. 33-41. doi: 10.15407/tdnk2017.02.05
12. Babak V., Zaporozhets A., Sverdlova A. Diagnostics of technical condition of thermal power objects based on distributed computing infrastructure. *Scientific Proceedings on HTCМ*. Vol. 187, №1, 2016, pp. 85-89.
13. Chiesa S., Fioriti M., Fusaro R. MALE UAV and its systems as basis of future definitions. *Aircraft Engineering and Aerospace Technology*. Vol. 88, Issue 6, 2016, pp. 771-782.
14. Anweiler S., Piwowarski D. Multicopter platform prototype for environmental monitoring. *Journal of Cleaner Production*. Vol. 155, Part 1, 2017, pp. 204-211. doi: 10.1016/j.jclepro.2016.10.132
15. Carlson J, Menicucci D., Vorobieff P., Mammoli A., He H. Infrared imaging method for flyby assessment of solar thermal panel operation in field settings. *Applied Thermal Engineering*. Vol 70, Issue 1, 2014, pp. 163-171. doi: 10.1016/j.applthermaleng.2014.05.008
16. Harvey M.C., Rowland J.V., Luketina K.M. Drone with thermal infrared camera provides high resolution georeferenced imagery of the Waikite geothermal area, New Zealand. *Journal of Volcanology and Geothermal Research*. Vol. 325, 2016, pp. 61-69. doi: 10.1016/j.jvolgeores.2016.06.014
17. Nishar A., Richards S., Breen D, Robertson J., Breen B. Thermal infrared imaging of geothermal environments and by an unmanned aerial vehicle (UAV): A case study of the Wairakei – Tauhara geothermal field, Taupo, New Zealand. *Renewable Energy*. Vol. 86, 2016, pp. 1256-1264. doi: 10.1016/j.renene.2015.09.042
18. Pajares G. Overview and Current Status of Remote Sensing Applications Based on Unmanned Aerial Vehicles (UAVs). *Photogrammetric Engineering & Remote Sensing*. Vol 81, Issue 4, 2015, pp. 281-329. doi: 10.14358/PERS.81.4.281
19. Tsanakas J.A., Ha L., Buerhop C. Faults and infrared thermographic diagnosis in operating c-Si photovoltaic modules: A review of research and future challenges. *Renewable and Sustainable Energy Reviews*. Vol. 62, 2016, pp. 695-709. doi: 10.1016/j.rser.2016.04.079

20. Yahyanejad S., Rinner B. A fast and mobile system for registration of low-altitude visual and thermal aerial images using multiple small-scale UAVs. *ISPRS Journal of Photogrammetry and Remote Sensing*. Vol. 104, 2015, pp. 189-202. doi: 10.1016/j.isprsjprs.2014.07.015
21. Kovacs M., Gaman G.A., Pupazan D., Calamar A., Irimia A. Research on the potentiality of using aerial vehicles for monitoring the environment agent – air. *Journal of Environmental Research and Protection*. Vol. 13, Issue 3, 2016, pp. 33-38.
22. Loginov I.D. Processing and segmentation of thermal images. *Young Scientist*. Vol. 147, №13, 2017, pp. 62-71.
23. Zaporozhets A.O., Kovtun S.I., Dekusha O.L. Determination of the technical condition of heat networks based on the processing of thermal imaging. *IEEE 14th International Scientific and Technical Conference on Computer Sciences and Information Technologies (CSIT)*. 2019 (in press)